

# Polyvinylidene Fluoride-Based Novel Polymer Electrolytes for Magnesium-Rechargeable Batteries with $\text{Mg}(\text{CF}_3\text{SO}_3)_2$

Vanchiappan Aravindan, G. Karthikaselvi, P. Vickraman, S. P. Naganandhini

Department of Physics, Gandhigram Rural University, Gandhigram 624302, India

Received 4 June 2008; accepted 9 December 2008

DOI 10.1002/app.29877

Published online 24 February 2009 in Wiley InterScience (www.interscience.wiley.com).

**ABSTRACT:** Magnesium trifluoromethanesulfonate ( $\text{Mg}(\text{CF}_3\text{SO}_3)_2$ )-based polymer electrolytes (PEs) have been prepared with polyvinylidene fluoride (PVdF) as a host matrix. Tetraglyme and tetrabutyl ammonium chloride (TBACl) were used as plasticizer and filler, respectively, in the matrix by solution-casting technique. The electrolyte containing 5 wt % TBACl exhibits the conductivity of  $0.442 \text{ mS cm}^{-1}$  at ambient temperature. X-ray diffraction study reveals the amorphous nature of the PE. Linear

sweep voltammetry was also performed to evaluate the decomposition potential of the electrolyte. The morphological features were analyzed by scanning electron microscope. The activation energy has also been calculated, which corroborates the ionic conductivity results. © 2009 Wiley Periodicals, Inc. *J Appl Polym Sci* 112: 3024–3029, 2009

**Key words:** magnesium batteries; tetraglyme; cyclic voltammetry; magnesium triflate; TBACl; PVdF

## INTRODUCTION

The successful commercialization of metallic lithium/insertion lithium ion-based primary and secondary batteries have explored the application of active materials as node with high energy density. The second interesting active material is zinc, which has also been widely used in the batteries. Another active material that attracts the researchers is magnesium, which is successfully employed as an electrode material in primary and reserve batteries. Recently, prototype magnesium-based rechargeable batteries have been demonstrated.<sup>1</sup> The rechargeable magnesium batteries are interesting when compared with lithium batteries because of the following advantages: (i) the ionic radii of  $\text{Li}^+$  and  $\text{Mg}^{2+}$  are 68 and 65 pm, respectively, hence  $\text{Li}^+$  can be easily replaced with  $\text{Mg}^{2+}$ ,<sup>2</sup> (ii) metallic magnesium is more stable than lithium, and therefore it can be handled in oxygen and humid atmospheres, (iii) terrestrial abundance of magnesium (1.94%) is plentiful than lithium (0.006%), thus it is much cheaper than lithium, (iv) comparable electrode potential (−3.05 and −2.38 V versus normal hydrogen electrode for  $\text{Li}^+$  and  $\text{Mg}^{2+}$  ions, respectively) and specific charge (3862 and 2205 A h  $\text{kg}^{-1}$  for  $\text{Li}^+$  and  $\text{Mg}^{2+}$ , respectively) with lithium.<sup>3</sup>

The key technology for developing highly reliable and safety is solid polymer electrolyte (PE) system with conducting  $\text{Mg}^{2+}$  species. Recently, Kumar and Munichandraiah<sup>4</sup> reported the reversibility  $\text{Mg}/\text{Mg}^{2+}$  couple in the PE gel systems. The conductivity of  $10^{-6}$  to  $10^{-4}$  were reported for the polyethylene oxide (PEO) : Mg complexes in the 80–100°C range, and the transport number of  $\text{Mg}^{2+}$  was found very low in these systems.<sup>5</sup> Polyacrylonitrile (PAN),<sup>6,7</sup> oligo(ethylene oxide)-grafted polymethacrylate (PEO-PMA),<sup>8</sup> polyethylene glycol (PEG)-borate ester,<sup>9</sup> and polymethylmethacrylate (PMMA)<sup>10</sup>-based systems were also investigated and excluded for the practical applications.

Recently, polyvinylidene fluoride (PVdF) was found to be very promising polymer matrix for the Mg-rechargeable batteries with tetraglyme (TG) as plasticizer. For using PVdF matrix, magnesium was reversibly deposited, with high ionic conductivity ( $\sim 10^{-3} \text{ S cm}^{-1}$ ) and wider electrochemical stability window in the presence of  $\text{Mg}(\text{AlCl}_2\text{EtBu})_2/\text{TG}$  at ambient temperature.<sup>11</sup> Furthermore, PEO-based system has also been investigated with same constituents, resulting in poor ionic conductivity and shorter electrochemical stability. The “glyme” family plasticizers, i.e., TG allows magnesium deposition and dissolution process in reversible manner without any surface film formation on the electrodes.<sup>11</sup> It was also found that, in contrast to lithium batteries, simple ionic salt solutions, i.e., polar solvents such as  $\text{Mg BF}_4^-$ ,  $\text{ClO}_4^-$ , and  $\text{PF}_6^-$  were impractical because of the reaction between active metal, i.e., magnesium, and the solution components.<sup>12</sup> This

Correspondence to: P. Vickraman (vrsvickraman@yahoo.com).

TABLE I  
Composition of Polymer Electrolytes

Sample	Polymer PVdF	Plasticizer TG	Mg Tf	TBACl
S1	30	65.0	5	0.00
S2	30	62.5	5	2.50
S3	30	60.0	5	5.00
S4	30	57.5	5	7.50
S5	30	55.0	5	10.0

work reports on the novel PEs based on magnesium trifluoromethanesulfonate ( $\text{Mg}(\text{CF}_3\text{SO}_3)_2$ ) as a salt, tetrabutyl ammonium chloride (TBACl) as a filler, and TG as plasticizer in PVdF matrix.

## MATERIALS AND METHODS

### Materials

PVdF and  $\text{Mg}(\text{CF}_3\text{SO}_3)_2$  (Mg Tf) were procured from Aldrich, USA. The plasticizer, TG, and the filler, TBACl, were obtained from Fluka and used as received. The solvent tetrahydrofuran (THF) was purchased from E. Merck, India, and used without further purification. A magnesium electrode was obtained from Ortal, Israel. The blending proportions employed for electrolyte fabrication are presented in Table I. The PEs were allowed to evaporate at room temperature, and the resulting membranes were kept under vacuum for about 10 h for further removal of the residual THF.

### Instrumentation

Ionic conductivities of the PEs were measured by a.c. impedance spectroscopy between 5 MHz and 1 Hz by using a Solartron 1260 Impedance/Gain Phase Analyzer coupled to a Solartron Electrochemical Interface. The conductivity cell had two stainless steel (SS) blocking electrodes and was of the configuration SS/PE/SS. The linear sweep voltammetry was used to determine the electrochemical stability of the PE. This was running a low scan (typically  $1 \text{ mV s}^{-1}$ ) in three electrode cells using "blocking type" working electrodes (e.g., SS) magnesium metal serves as both counter and pseudoreference electrode, and the given membrane sample act as electrolyte. The coherence length was calculated using the following relation:

$$L = \frac{0.9\lambda}{\Delta 2\theta_b \cos \theta_b} \quad (1)$$

where  $\lambda$  is the X-ray wavelength,  $\Delta 2\theta_b$  is the full width at half maximum, and  $\theta_b$  is the angle of the peak.

## RESULTS AND DISCUSSION

### Alternating current impedance analysis

Electrochemical impedance spectroscopy is a powerful tool for examining many chemical and physical processes in solutions as well as solids. This technique has grown tremendously in stature over the past few years and is now being widely employed in a variety of scientific fields such as batteries, fuel cell testing, biomolecular interaction, microstructural characterization, etc. The ionic conductivities of PEs are calculated from the following equation:

$$\sigma = \frac{l}{R_b r^2 \pi} \quad (2)$$

where  $l$  and  $r$  represent the thickness and radius of the sample membrane disk, respectively.  $R_b$  is the bulk resistance obtained from a.c. impedance measurements.<sup>13</sup> It is observed that the addition of TBACl substantially enhances the conductivity (Fig. 1). It could be found that the substantial increase in conductivity is accomplished for 5 wt % TBACl content, and the conductivity tends to decrease beyond 5 wt %. However, a slight increase in conductivity is observed for 10 wt % filler containing PE.

In this study, the conductivity enhancement could be well observed for the lower filler concentration, which might be due to the uniform dispersion of filler throughout the volume. The reverse trend is observed for 5–7.5 wt %, which might be due to the blocking effect that leads to immobilize the polymer chains causing dropping in the conductivity. Furthermore, by increasing the filler content, the filler grains get closer enough to each other so that the high conducting regions in the vicinity of the grain surfaces start to get interconnected. Then, the

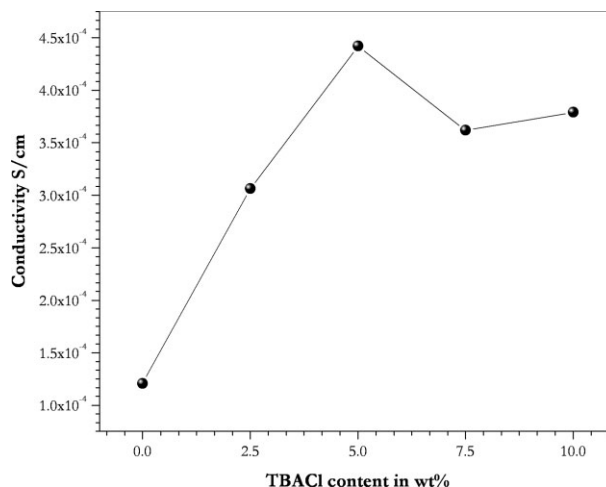
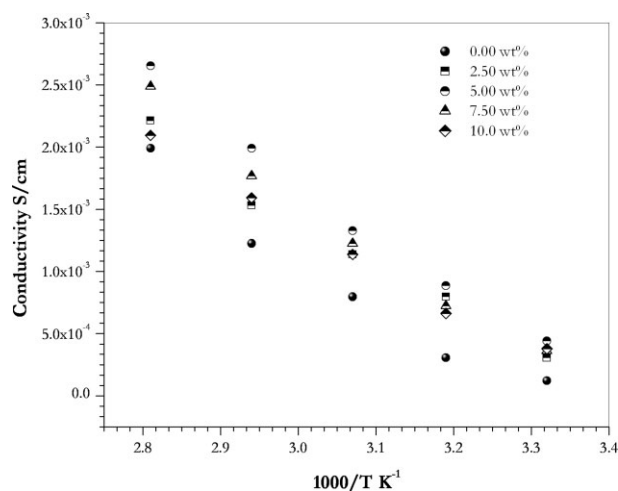


Figure 1 Variation of ionic conductivity with different TBACl concentrations.



**Figure 2** Temperature dependency of the magnesium polymer electrolytes.

migration of ionic species can thus travel along, and between these interconnected and high conducting pathways it give rise to the increase in conductivity beyond 7.5 wt %.<sup>14</sup> The temperature dependency on ionic conductivity is presented in Figure 2. The behavior of the ionic conduction in the PE obeys the Vogel-Tamman-Fulcher (VTF) relation, which describes the transport properties in a viscous polymer matrix.<sup>15</sup>

### Activation energy for $\text{Mg}^{2+}$ ion transport

Figure 2 depicts the dependence of ionic conductivity on temperature in the range 27–70°C. The activation energy for ion transport,  $E_a$  is obtained by using the following VTF model:

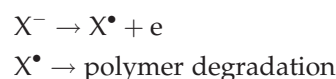
$$\sigma = \sigma_0 T^{-1/2} \exp\left(\frac{-E_a}{T - T_0}\right) \quad (3)$$

where  $\sigma$  is the conductivity,  $\sigma_0$  is the preexponential factor,  $T_0$  is the glass transition temperature, and  $T$  is the temperature. Figure 3 shows the relationship between the amount of TBACl in the polymer film and the activation energy for ion transport. It is found that the activation energy for ion transport decreases up to 5 wt % filler particles. However, activation energy increases beyond this concentration. The minimum activation energy is found to be  $1.79 \text{ kJ mol}^{-1}$  for 5 wt % filler concentration.

### Electrochemical stability

The electrochemical stability of the magnesium-based membranes were evaluated by running a linear sweep voltammetry on a cell using a blocking, SS working electrode, and magnesium counter elec-

trode. The anodic onset of the current is detected around 1.75 V, which is assumed as the membrane decomposition voltage, i.e., a value high enough to allow safe usage of the PE in connection with magnesium ion electrode coupling thereby typically cycled around 1.2–1.5 V. The occurrence of reversible cathodic peak around 0 V, due to the magnesium deposition process on the SS electrode, shows the applicability of these membranes in Mg-based rechargeable batteries. Bonino et al.<sup>16</sup> suggests that PE decomposition occurs in this potential range by the following process:



where  $X^-$  is the electrolyte anion. The enhancement of such stability may attribute to the good porosity with high surface area and good affinity of PVdF with liquids, i.e., TG. The observed very small current limit between the two limits is the clear indication of purity and integrity of the membrane. The observed anodic current has been reduced from 19 to 16 mA due to the addition of fillers into the pure membrane, which confirms the passivation of surface films on the electrode as it is hindered by TBACl.<sup>17</sup> The TBACl also enhances the kinetics of the Mg deposition/dissolution process, which could be clearly seen in Figure 4. A similar type of faster kinetics was observed by Gofer et al.<sup>18</sup> after the incorporation of TBACl into magnesium organo-halo-aluminates.

### X-ray diffraction analysis

X-ray diffraction measurements were made to examine the crystallinity of the PEs. PVdF exists in four

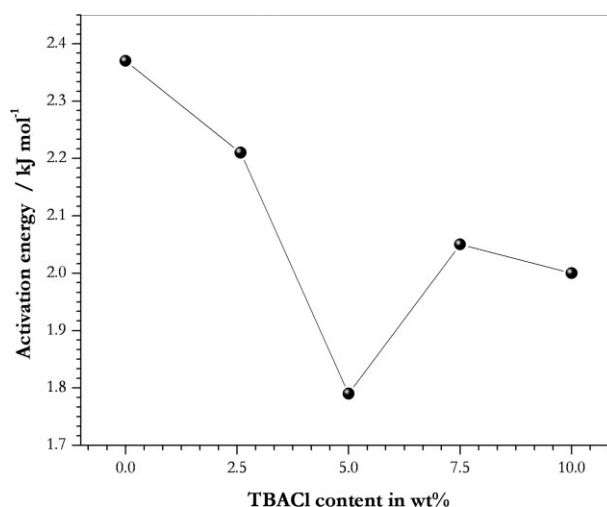


**Figure 3** Activation energy for  $\text{Mg}^{2+}$  ion transport with different TBACl concentrations.

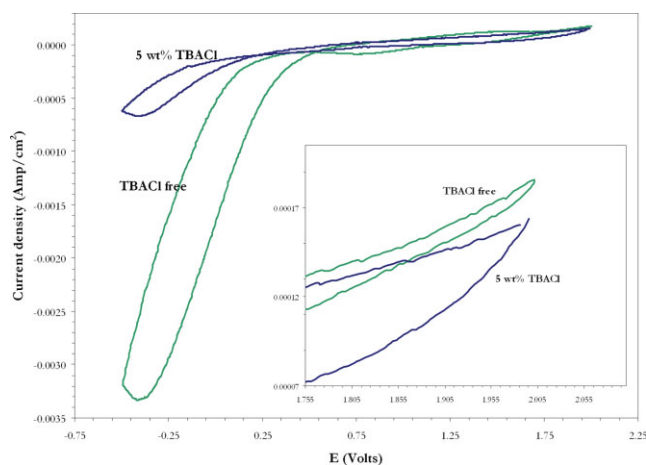


**Figure 4** Linear sweep voltammogram depicts magnesium polymer electrolytes of the Mg/polymer electrolyte/SS at room temperature. [Color figure can be viewed in the online issue, which is available at [www.interscience.wiley.com](http://www.interscience.wiley.com).]

crystalline phases, namely  $\alpha$ ,  $\beta$ ,  $\gamma$ , and  $\delta$  phases. Generally, XRD patterns of PVdF show some characteristic peaks at  $2\theta \approx 17.6^\circ$ ,  $26.7^\circ$ , and  $38.7^\circ$  corresponding to big spherulites of VdF  $\alpha$ -phase crystals [(1 0 0), (0 2 1), and (1 3 1) planes, respectively], and spherulites of VdF  $\gamma$ -phase crystals may coexist with the  $\alpha$ -phase crystals at  $2\theta \approx 18^\circ$  and  $21^\circ$  [(0 2 0) and (1 1 0) planes, respectively] (Fig. 5).<sup>19</sup> It is seen from XRD pattern that except  $2\theta \approx 21^\circ$ , all the characteristics peaks of PVdF are absent in the electrolytes suggesting the formation of amorphous phase, which is reflected in the ionic conductivity measurement and also in the activation energy calculations. The absence of  $\alpha$ -phase crystal structure at  $2\theta \approx 18^\circ$  may be inferred that the addition of fillers induces the structural change of  $\beta$ -phase form to  $\alpha$ -phase.<sup>20</sup> The suppression of these peaks may be due to the addition of plasticizers and TBACl, which strongly interact with polymer host and increases the flexibility of

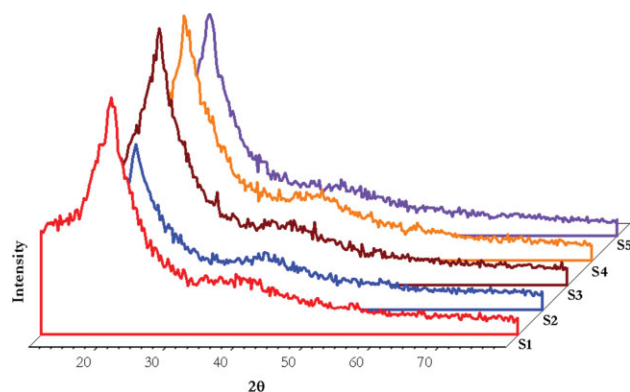


**Figure 5** X-ray diffractograms of magnesium polymer electrolytes. [Color figure can be viewed in the online issue, which is available at [www.interscience.wiley.com](http://www.interscience.wiley.com).]

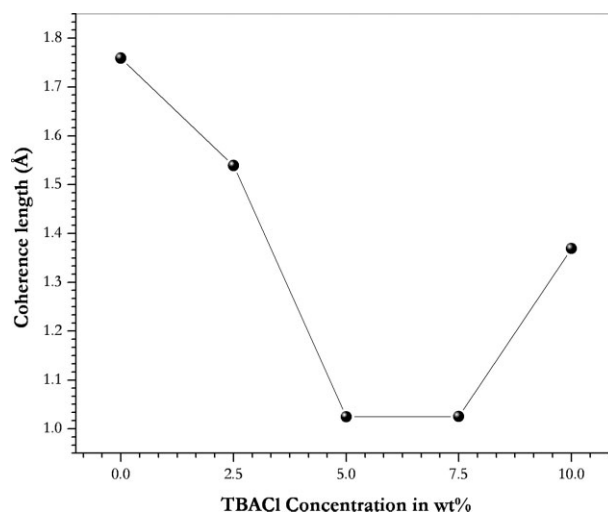


**Figure 6** Coherence length ( $2\theta \approx 21^\circ$ ) of the polymer electrolyte.

the polymer chains as it is the case of semicrystalline nature of the host.

The coherence length of the electrolytes has also been calculated for  $2\theta \approx 21^\circ$  to find the amorphousness of the film. Figure 6 presents the coherence length of the magnesium PEs. The 5 wt % TBACl containing electrolyte shows shortest coherence length [1.0248 Å, which is slightly lower than 7.5 wt % containing electrolytes (1.0253 Å)] and the rest of the electrolytes showed much longer coherence than the former, and these coherence length variations are in tune with the conductivity measurement.<sup>21</sup>

### Morphological studies

The morphological features are analyzed by SEM (Fig. 7). With the addition of small amount of TBACl (i.e., 2.5 wt %) into the pure electrolyte, the morphology drastically changes, i.e., phase separation has occurred. The increase in phase separation is observed for 5 wt % TBACl containing electrolyte. It could be well observed that smooth surface and large number of voids are present in the system. These small pores are necessary for the transportation of  $Mg^{2+}$  from cathode to anode and vice versa.<sup>14</sup> The phase separation is not clearly observed when TBACl content exceeds 5 wt %, which may be due to the aggregation of filler content changing the morphology of the electrolyte. The flake-like appearance is clearly seen for high-loading TBACl (10 wt %) of fillers.

### CONCLUSION

The Mg Tf-based electrolyte with 5 wt % TBACl gave an ambient temperature conductivity of 4.42 ×

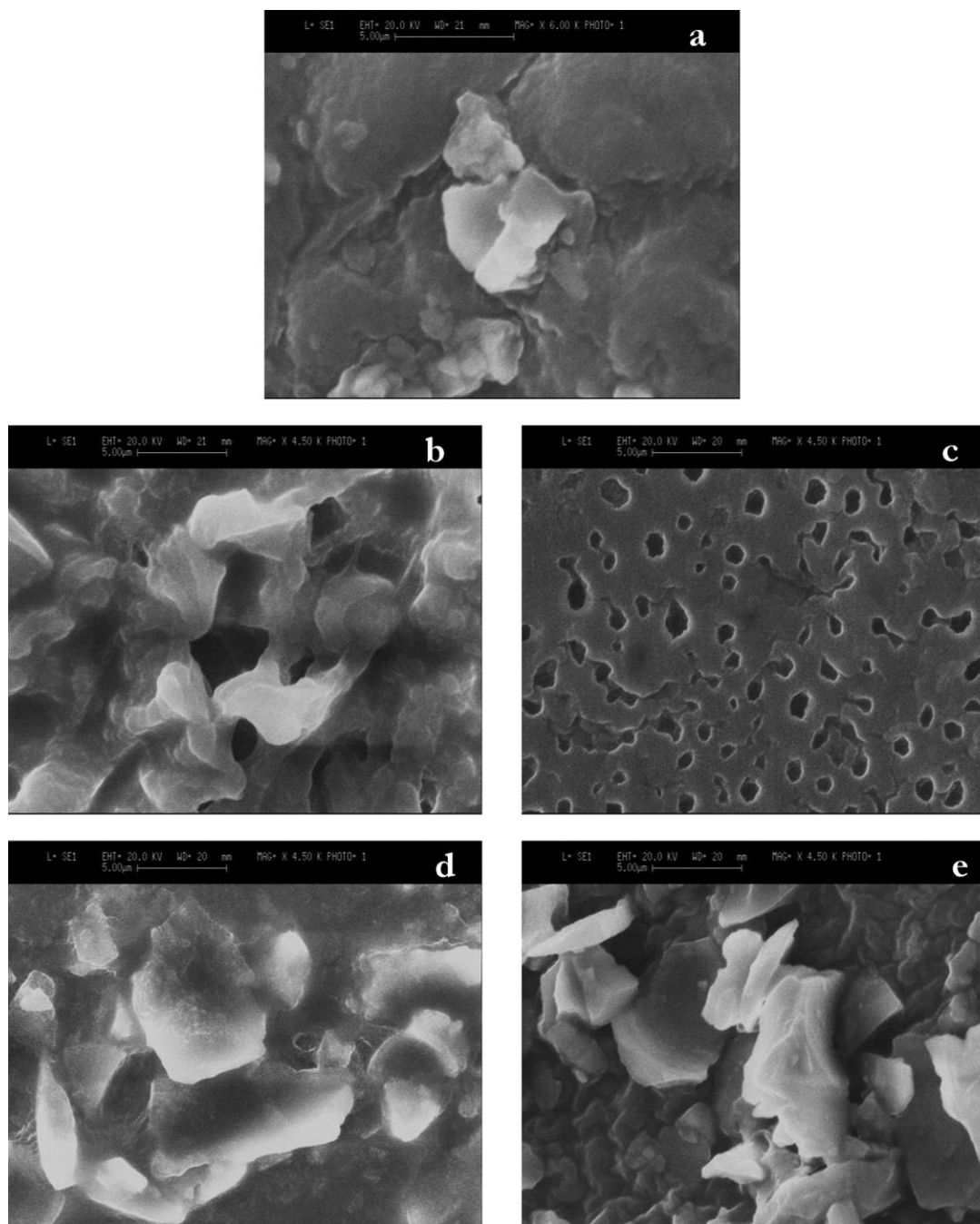


**Figure 7** Scanning electron microscopic images of magnesium polymer electrolytes with (a) 0, (b) 2.5, (c) 5.0, (d) 7.5, and (e) 10 wt % of TBACI concentration.

$10^{-4} \text{ S cm}^{-1}$  and possessed a nearly uniform porous network for the accommodation of large amounts of liquid electrolyte in it. The high conductivity of the electrolyte is attributed to its high amorphicity, which facilitates a high mobility of  $\text{Mg}^{2+}$  ions by the way of large free volumes. The addition of TBACI not only enhances the conductivity but also enhances the kinetics of the  $\text{Mg}^{2+}$  ion intercalation. Thus, this membrane is a potential candidate for Mg-rechargeable batteries.

One of the authors (V. A.) is grateful to Ortal Diecasting Incorporation, Israel, for gratis providing magnesium electrodes. The authors also thank Mrs. Anna Maria Bertasa, Solvay Solexis S.p.A., Italy, for providing the research materials.

#### References

1. Aurbach, D.; Lu, Z.; Schechter, Y.; Gizbar, H.; Turgeman, R.; Cohen, Y.; Moshkovich, M.; Levi, E. *Nature* 2000, 274, 724.
2. Novak, P.; Imhof, R.; Haas, O. *Electrochim Acta* 1999, 44, 351.

3. Besenhard, J. O.; Winter, M. *Chem Phys Chem* 2002, 3, 155.
4. Kumar, G. G.; Munichandraih, N. *Electrochim Acta* 1999, 44, 2663.
5. Gray, F. M. *Solid Polymer Electrolyte*; VCH: New York, 1991; Chapter 7.
6. Kumar, G. G.; Munnichandraiah, N. *J Power Sources* 2000, 91, 157.
7. Perera, K.; Dissanayake, M. A. K. L.; Bandaranayake, P. W. S. *K. Mater Res Bull* 2004, 39, 1745.
8. Morita, M.; Yoshimoto, N.; Yakushiji, S.; Ishikawa, M. *Electrochem Solid-State Lett* 2001, 4, A177.
9. Saito, M.; Ikuta, H.; Uchimoteo, Y.; Wakihara, M.; Yokoyama, S.; Yabe, T.; Yamamoto, M. *J Electrochem Soc* 2003, 150, A447.
10. Kumar, G. G.; Munichandraih, N. *Electrochim Acta* 2002, 47, 1013.
11. Chusid, O.; Gofer, Y.; Gizbar, H.; Vestfried, Y.; Levi, E.; Aurbach, D.; Riech, I. *Adv Mater* 2003, 15, 627.
12. Aurbach, D.; Weissman, I.; Gofer, Y.; Levi, E. *Chem Rec* 2003, 3, 61.
13. Available at <http://www.solartronanalytical.com/technicalsupport/technicalnotes/technote31.htm>.
14. Aravindan, V.; Vickraman, P. *J Phys D: Appl Phys* 2007, 40, 6754.
15. Wang, H.; Huang, H.; Wunder, S. L. *J Electrochem Soc* 2000, 147, 2853.
16. Bonino, F.; Scrosati, B.; Selvaggi, A. *Solid-State Ionics* 1986, 18, 1050.
17. Zhou, Z. B.; Takeda, M.; Fuji, T.; Ue, M. *J Electrochem Soc* 2005, 152, A351.
18. Gofer, Y.; Chusid, O.; Gizbar, H.; Vestfried, Y.; Gottlieb, H. E.; Marks, V.; Aurbach, D. *Electrochem Solid-State Lett* 2006, 9, A257.
19. Marand, H. L.; Stein, R. S.; Stack, G. M. *J Polym Sci Part B: Polym Phys* 1988, 26, 1361.
20. Aravindan, V.; Vickraman, P.; Krishnaraj, K. *Polym Int* 2008, 57, 932.
21. Mohamed, N. S.; Zakaria, M. S.; Ali, A. M. M.; Arof, A. K. *J Power Sources* 1997, 66, 169.